

# Theoretical study of the decomposition of ethyl and ethyl 3-phenyl glycidate

Daniela Josa · Angeles Peña-Gallego ·  
Jesús Rodríguez-Otero · Enrique M. Cabaleiro-Lago

Received: 14 May 2012 / Accepted: 23 July 2012 / Published online: 14 August 2012  
© Springer-Verlag 2012

**Abstract** The mechanism of the decomposition of ethyl and ethyl 3-phenyl glycidate in gas phase was studied by density functional theory (DFT) and MP2 methods. A proposed mechanism for the reaction indicates that the ethyl side of the ester is eliminated as ethylene through a concerted six-membered cyclic transition state, and the unstable intermediate glycidic acid decarboxylates rapidly to give the corresponding aldehyde. Two possible pathways for glycidic acid decarboxylation were studied: one via a five-membered cyclic transition state, and the other via a four-membered cyclic transition state. The results of the calculations indicate that the decarboxylation reaction occurs via a mechanism with five-membered cyclic transition state.

**Keywords** Ethyl glycidate · Ethyl 3-phenyl glycidate · Ab initio calculation · DFT calculation · Reaction mechanism

## Introduction

One of the most important transformations of glycidic esters is their decarboxylation to give aldehydes and ketones (Reaction 1). Various methods for this conversion have been studied experimentally [1–5]. However, an accurate description of this mechanism is challenging, since the glycidic acid intermediate decomposes even at room temperature.

D. Josa · A. Peña-Gallego (✉) · J. Rodríguez-Otero  
Centro Singular de Investigación en Química Biolóxica e Materiais Moleculares (CIQUS), Universidade de Santiago de Compostela, Rúa Jenaro de la Fuente, s/n, Santiago de Compostela 15782, Spain  
e-mail: angeles.pena@usc.es

E. M. Cabaleiro-Lago  
Departamento de Química Física, Facultad de Ciencias, Universidade de Santiago de Compostela, Av. Alfonso X o Sabio, s/n, Lugo 27002, Spain

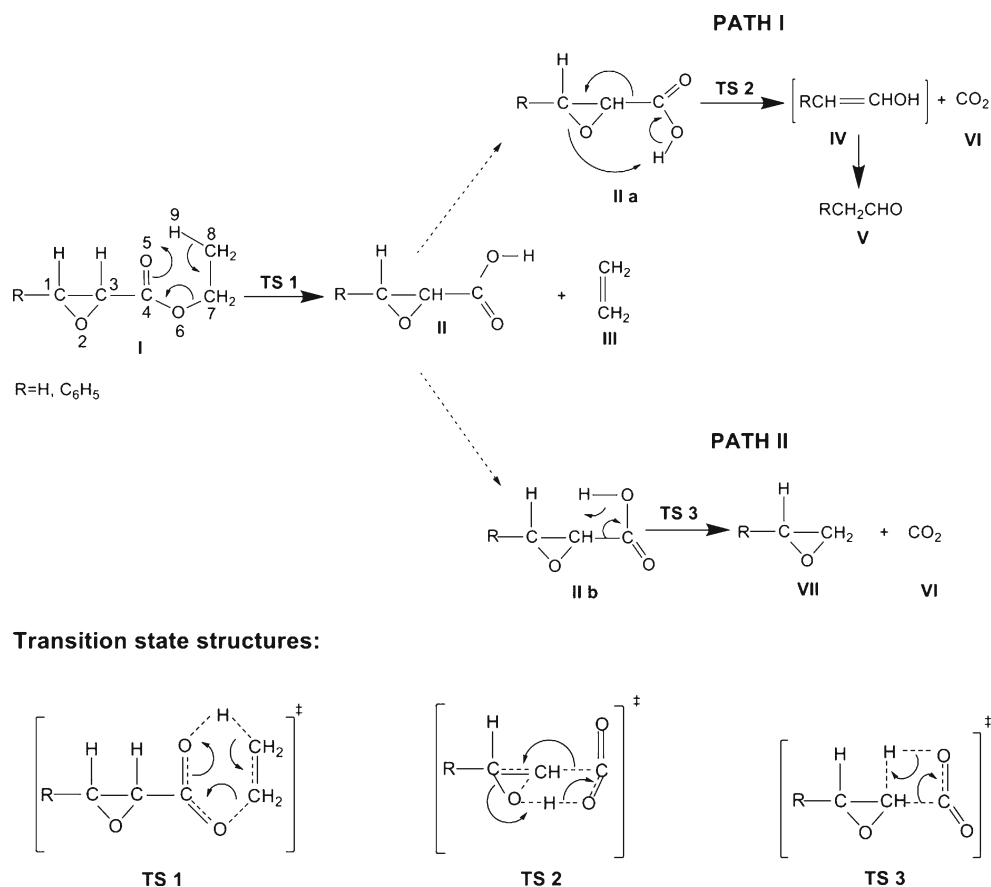
According to experimental studies performed by Chuchani and co-workers [6], the decomposition reaction of ethyl 3-phenyl glycidate is homogeneous, unimolecular and obeys a first-order rate law. The results of this investigation indicate that the reaction occurs in two steps: the first involves the elimination of the alkyl side of the ester through a concerted six-membered cyclic transition state; the second involves decarboxylation of glycidic acid. Two pathways were proposed for this second step: either via a five-membered cyclic transition state (Fig. 1, TS2) or a four-membered cyclic transition state (Fig. 1, TS3) [6].

In reaction mechanisms with similar steps, such as in the elimination of ethyl carbonates [7] and ethyl carbamates [8–10], the decarboxylation process occurs via a four-membered cyclic transition state. However, according to experimental results, a four-membered cyclic transition state appears to be unlikely for the glycidic acid studied because the epoxy intermediate has not been isolated. A mechanism suggested for decarboxylation indicates that carbon at the 3-position, rather than carbon at the 2-position, is more liable to C–O bond polarization, in the sense of  $C^{\delta+}\cdots O^{\delta-}$ . So, the oxygen becomes very nucleophilic and may abstract the hydrogen of the COOH through a five-membered cyclic transition state to yield 2-phenylacetaldehyde and carbon dioxide (Fig. 1, TS2) [6].

The final product obtained from decarboxylation of glycidic acid, i.e., 2-phenylacetaldehyde, is an important intermediate used in the preparation of the novel active substances of insecticides, herbicides, fungicides, and medicines [11]. It is also found in many foods and flowers [12, 13].

Although the studies performed by Chuchani et al. [6] allow us to rationalize a mechanism for the decarboxylation of glycidic acid, a detailed study of the mechanism taking into account the two possible pathways for the glycidic acid decarboxylation to confirm their experimental hypothesis is necessary.

**Fig. 1** Two mechanisms proposed for the decomposition of ethyl and ethyl 3-phenyl glycidate. IIa and IIb correspond to the reactive conformation of the 3-phenylglycidic acid for paths I and II, respectively



Therefore, the goal of this work was to perform an accurate theoretical study of the decomposition of ethyl 3-phenyl glycidate in order to explore the nature of the reaction mechanism. Geometries of the different reactants, products and intermediates were optimized at different levels of calculation. The vibrational frequencies were calculated at the same level. Intrinsic reaction coordinate (IRC) calculations were performed and the progress of the reaction was followed by employing the Wiberg bond indices [14]. Activation energies and Gibbs free energies of activation were also analyzed.

### Computational details

The mechanisms of decomposition of ethyl and ethyl 3-phenyl glycidate in the gas phase were investigated by means of electronic structure calculations. The geometry of each stationary point corresponding to reactants, products, and transition states was optimized employing second-order Møller-Plesset theory (MP2) or DFT using the B3LYP functional.

Other studies [15] indicate an important improvement in results when adding diffuse functions. Therefore, all calculations in this work include diffuse functions. The 6-31+G\*, 6-31++G\*\*, aug-cc-pVDZ and aug-cc-pVTZ basis set were employed in the calculations.

Single point calculations at the MP4 and CCSD(T) levels were also performed for selected conformations in the study of the decomposition of ethyl glycidate.

All points were characterized as minima or transition structures by calculating the harmonic frequencies and forces constants, using analytical second derivatives. Zero point-energy (ZPE) corrections were included in the calculations.

IRC calculations [16] were also performed to follow the reaction path in both directions from transition states at the B3LYP/6-31+G\* level of theory.

The activation energy was obtained using the following equations:

$$E_a = \Delta H^\ddagger(T) + RT \quad (1)$$

$$\Delta H^\ddagger = \Delta H_{TS} - \Delta H_{react} \quad (2)$$

where  $\Delta H_{TS}$  and  $\Delta H_{react}$  are the enthalpies for the transition state and the reactants (reactive conformation), respectively.  $R$  represents the universal gas constant ( $1.9872 \text{ cal mol}^{-1} \text{ K}^{-1}$ ), and  $T$  represents the temperature (we have used a value of 643.15 K, temperature where there are experimental kinetic data) [6].

Natural bond orbital (NBO) analysis was performed using the NBO program implemented in the Gaussian03 program package [17] to follow the progress of the reactions and investigate the bonding characteristics. All calculations were carried out using the Gaussian03 program package [17].

## Results and discussion

The mechanism proposed in experimental studies [6] for the reaction of the decomposition of ethyl 3-phenyl glycidate in the gas phase is given in Fig. 1. The reaction has two steps: the first process occurs via a six-membered cyclic transition state (TS1) and the second can occur via a five- or four-membered cyclic transition state, given as TS2 and TS3, respectively [6]. These two possible pathways for the decomposition of ethyl 3-phenyl glycidate were investigated in this work.

Several optimizations using different starting points were performed at the MP2/6–31+G\* level to obtain the ethyl glycidate minima. Figure 2 shows the geometries for the two most important located minima.

The minimum II, with a planar skeleton, corresponds to the most stable structure, although the difference (ZPE) with minimum I is very small—only 0.2 kcal mol<sup>-1</sup>. Minimum I was used in the following calculations due to its more favorable geometry for the elimination of the alkyl side of the ester through a concerted six-membered cyclic transition state; it is the reactive conformation.

The calculated activation energy and Gibbs free energy of activation for the transition states analyzed are summarized in Table 1. The calculations were performed at the same temperature used in the experiments, 643.15 K [6]. The calculated values of the activation energy and Gibbs free energy of activation for the decomposition of ethyl 3-phenyl glycidate agree well with experimental data [6]. The

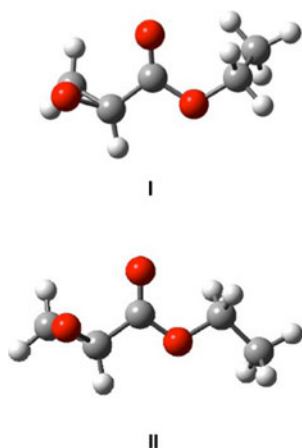


**Fig. 2** Geometry of ethyl glycidate minima at the MP2/6–31+G\* level

activation energy shows values in the range from 44.7 to 52.7 kcal mol<sup>-1</sup> and Gibbs free energy of activation from 43.6 to 51.7 kcal mol<sup>-1</sup>, while 45.4 and 48.3 kcal mol<sup>-1</sup>, respectively, were obtained from experiments [6].

It can be seen from Table 1 that the reaction of ethyl glycidate and ethyl 3-phenyl glycidate, despite having similar TS1 activation energy values, shows significant differences in TS2 values. The introduction of a phenyl group in the 3-position in ethyl glycidate provides a stabilization of 17.4 kcal mol<sup>-1</sup> for TS2 activation energy at the MP2/6–31+G\* level. This result may be due to a stabilization of the carbocation character of the carbon at the 3-position of the glycidic acid intermediate by resonance. The  $\pi$  electrons of the phenyl group help delocalize the positive charge, increasing stability. Therefore, the rate-determining step for the decomposition of ethyl 3-phenyl glycidate is TS1, while TS2 is the rate-determining step in the decomposition of ethyl glycidate

The optimized transition structures for the decomposition of ethyl 3-phenyl glycidate are given in Fig. 3.

A comparison of the results at different calculation levels given in Table 1 provides observations similar to those obtained in the theoretical study of the thermal elimination of ethyl formate [15]. Therefore, our results confirm that the previous study employing the small molecule of ethyl formate at different level calculations is a good reference for theoretical studies of similar molecules.

The free energy profile for the process of decomposition of ethyl 3-phenyl glycidate is depicted in Fig. 4. It can be clearly observed that the second step of the mechanism occurs via a five-membered cyclic transition state (TS2). The other pathway with a four-membered cyclic transition state (TS3) shows a activation free energy 22.4 kcal mol<sup>-1</sup> higher than the corresponding values for TS2 at the MP2/6–31+G\* level. Our theoretical results confirm the previous experimental hypothesis that the second step of the mechanism occurs by a five-membered cyclic transition state [6].

Wiberg bond indices [14] were computed to obtain a detailed analysis of the progress of the reaction. Table 2 summarizes the Wiberg bond indices corresponding to the bonds involved in the reaction center for the rate-determining step of the decomposition of ethyl and ethyl 3-phenyl glycidate.

The bond breaking and bond forming process along the reaction path can be analyzed by employing the synchronicity ( $S_y$ ) concept proposed by Moyano et al. [18] The synchronicity values vary between zero and one. A value of one indicates that all bonds involved in the reaction have broken or formed to exactly the same extent in the transition state.  $S_y$  can be calculated by means of the expression:

$$S_y = 1 - A \quad (3)$$

**Table 1** Activation energy ( $E_a$ ) and Gibbs free energy of activation ( $\Delta G^\ddagger$ , in kcal mol<sup>-1</sup>) at 643.15 K for the decomposition of ethyl and ethyl 3-phenyl glycidate at different calculation levels. Experimental data is given for decomposition of ethyl 3-phenyl glycidate

| Geometry and vibrational calculation | Single point energy | TS1   |                     | TS2   |                     | TS3   |                     |
|--------------------------------------|---------------------|-------|---------------------|-------|---------------------|-------|---------------------|
|                                      |                     | $E_a$ | $\Delta G^\ddagger$ | $E_a$ | $\Delta G^\ddagger$ | $E_a$ | $\Delta G^\ddagger$ |
| Ethyl glycidate                      |                     |       |                     |       |                     |       |                     |
| B3LYP/6-31+G*                        | B3LYP/6-31+G*       | 46.8  | 45.4                | 49.6  | 48.4                | 66.0  | 64.5                |
| B3LYP/6-31++G**                      | B3LYP/6-31++G**     | 44.6  | 43.4                | 49.0  | 48.0                | 65.4  | 64.0                |
| MP2/6-31+G*                          | MP2/6-31+G*         | 52.6  | 51.7                | 60.3  | 58.8                | 67.8  | 66.6                |
|                                      | MP4/6-31+G*         | 51.8  | 55.6                | 55.2  | 49.7                | 67.9  | 71.3                |
| MP2/aug-cc-pVDZ                      | MP2/aug-cc-pVDZ     | 48.3  | 47.4                | 58.5  | 57.3                | 64.5  | 63.1                |
|                                      | MP4/aug-cc-pVDZ     | 47.7  | 51.1                | 53.3  | 55.2                | 64.5  | 67.8                |
|                                      | MP4/aug-cc-pVTZ     | 48.4  | 51.9                | 55.0  | 56.9                | 63.9  | 67.2                |
|                                      | CCSD(T)/aug-cc-pVDZ | 48.7  | 55.5                | 53.5  | 55.5                | 68.2  | 71.5                |
| Ethyl 3-phenyl glycidate             |                     |       |                     |       |                     |       |                     |
| B3LYP/6-31+G*                        | B3LYP/6-31+G*       | 46.9  | 45.5                | 32.1  | 32.6                | 64.0  | 62.9                |
| B3LYP/6-31++G**                      | B3LYP/6-31++G**     | 44.7  | 43.6                | 31.4  | 31.9                | 64.2  | 62.7                |
| MP2/6-31+G*                          | MP2/6-31+G*         | 52.7  | 51.7                | 42.9  | 42.8                | 66.5  | 65.2                |
| Experimental (643.15 K) [6]          |                     | 45.4  | 48.3                |       |                     |       |                     |

where  $A$  is the asynchronicity, calculated as:

$$A = \frac{1}{(2N - 2)} \sum \frac{|\delta B_i - \delta B_{av}|}{\delta B_{av}} \quad (4)$$

and where  $n$  is the number of bonds directly involved in a reaction chemical.

The relative variation of bond index is given by:

$$\delta B_i = \frac{(B_i^{TS} - B_i^R)}{(B_i^P - B_i^R)} \quad (5)$$

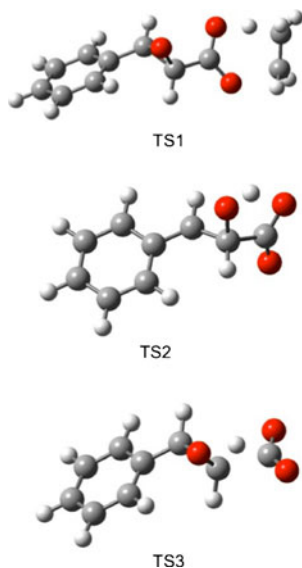


**Fig. 3** MP2/6-31+G\* geometry of the transition states; TS1 corresponding to the first step of the decomposition of ethyl 3-phenyl glycidate, TS2 and TS3 correspond to path I and path II for the second step of the mechanism, respectively

The percentage evolution (%EV) [19] of the bond order is calculated as:

$$\%EV = 100\delta B_i \quad (6)$$

The average value,  $\delta B_{av}$ , is obtained from:

$$\delta B_{av} = \frac{1}{n} \sum \delta B_i \quad (7)$$

The calculated Wiberg bond indices for the rate-determining step for the decomposition of ethyl 3-phenyl glycidate indicate a more advanced progress in the O<sub>6</sub>-C<sub>7</sub> bond breaking (63 %) and less progress in the C<sub>7</sub>-C<sub>8</sub> double bond formation (39 %).

The synchronicity value of the 0.92, indicates a slightly asynchronous process. The charge distribution in reactants and transition states obtained in the NBO analysis results are given in Table 3.

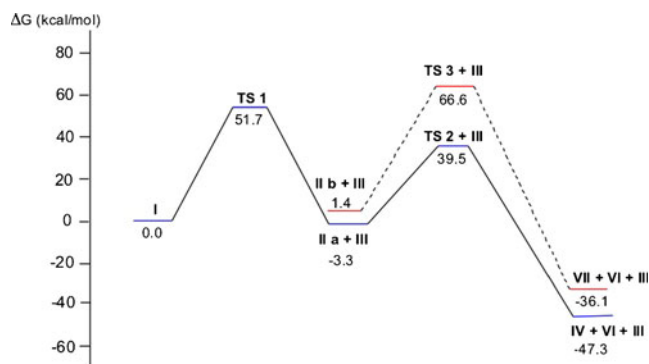


**Fig. 4** Gibbs free energy for the decomposition of ethyl 3-phenyl glycidate at the MP2/6-31+G\* level. IIa and IIb corresponds to the reactive conformation of the 3-phenylglycidic acid for path I (solid line) and path II (dashed line), respectively

**Table 2** Wiberg bond indices ( $B_i$ ) of reactants, transition states and products for the rate-determining step of the reaction of the decomposition of ethyl and ethyl 3-phenyl glycidate, percentage of evolution (%EV) through the chemical process of the bond indices at the transition states, degree of advancement of transition states ( $\delta B_{av}$ ), and absolutes synchronicities ( $S_y$ ). Values obtained at B3LYP/6–31+G\* level

| Analysis of the progress of the reaction |                                |                                |                                |                                |                                |                                |                 |       |
|--|--------------------------------|--------------------------------|--------------------------------|--------------------------------|--------------------------------|--------------------------------|-----------------|-------|
| Ethyl glycidate                          |                                |                                |                                |                                |                                |                                |                 |       |
|  | C <sub>1</sub> -O <sub>2</sub> | O <sub>2</sub> -H <sub>9</sub> | H <sub>9</sub> -O <sub>5</sub> | O <sub>5</sub> -C <sub>4</sub> | C <sub>4</sub> -C <sub>3</sub> | C <sub>3</sub> -C <sub>1</sub> | $\delta B_{av}$ | $S_y$ |
| $B_i^R$                                  | 0.90                           | 0.03                           | 0.68                           | 1.06                           | 0.96                           | 0.99                           | 0.49            | 0.75  |
| $B_i^{TS2}$                              | 0.42                           | 0.56                           | 0.14                           | 1.43                           | 0.75                           | 1.18                           |                 |       |
| $B_i^P$                                  | 0.00                           | 0.73                           | 0.00                           | 1.89                           | 0.00                           | 1.91                           |                 |       |
| %EV                                      | 53.3                           | 75.7                           | 79.4                           | 44.6                           | 21.9                           | 20.6                           |                 |       |
| Ethyl 3-phenyl glycidate                 |                                |                                |                                |                                |                                |                                |                 |       |
|  | O <sub>5</sub> -C <sub>4</sub> | C <sub>4</sub> -O <sub>6</sub> | O <sub>6</sub> -C <sub>7</sub> | C <sub>7</sub> -C <sub>8</sub> | C <sub>8</sub> -H <sub>9</sub> | H <sub>9</sub> -O <sub>5</sub> | $\delta B_{av}$ | $S_y$ |
| $B_i^R$                                  | 1.74                           | 1.05                           | 0.85                           | 1.03                           | 0.92                           | 0.00                           | 0.51            | 0.92  |
| $B_i^{TS1}$                              | 1.36                           | 1.43                           | 0.31                           | 1.42                           | 0.45                           | 0.29                           |                 |       |
| $B_i^P$                                  | 1.06                           | 1.77                           | 0.00                           | 2.04                           | 0.00                           | 0.68                           |                 |       |
| %EV                                      | 55.9                           | 52.8                           | 63.5                           | 38.6                           | 51.1                           | 42.6                           |                 |       |

It can be seen that there is a significant positive charge developed in the transition states compared with reactants on H<sub>9</sub> (from 0.25 in R to 0.42 in TS) and an increase in the negative charge of O<sub>5</sub> (from -0.60 in R to -0.68 in TS). This negative character of O<sub>5</sub> allows H<sub>9</sub> abstraction in the transition state, and an increase in the negative charge in O<sub>6</sub> (from -0.55 in R to -0.63 in TS) following the breaking of the O<sub>6</sub>-C<sub>7</sub> bond. The results indicate that polarization of the O<sub>6</sub>-C<sub>7</sub> bond is an important factor in the decomposition of ethyl 3-phenyl glycidate.

The reaction of decomposition of ethyl glycidate with a five-membered cyclic transition state show more advanced progress in H<sub>9</sub>-O<sub>5</sub> bond breaking (79 %). The bond formation of O<sub>2</sub>-H<sub>9</sub> (76 %) also shows a very large progress in the reaction mechanism. Therefore, the results indicate that the transference of H<sub>9</sub> is the most important process in the mechanism of decomposition of ethyl glycidate. The breaking of the C<sub>3</sub>-C<sub>1</sub> and C<sub>4</sub>-C<sub>3</sub> bonds are the less advanced processes. This mechanism shows a synchronicity value of 0.75, indicating a more asynchronous process compared with the mechanism of the decomposition of the ethyl 3-

phenyl glycidate. NBO charge analysis reveals that C<sub>1</sub> becomes more positive in the transition state (from -0.13 in R to -0.01 in TS), while C<sub>3</sub> becomes more negative (from -0.07 in R to -0.14 in TS). Therefore, the results indicate that C<sub>1</sub> and not C<sub>3</sub> is responsible for the increase in O<sub>2</sub> nucleophilicity (from -0.55 in R to -0.64 in TS) to allow the abstraction of H<sub>9</sub> of the COOH, in agreement with the results rationalized by Chuchani et al. [6] for 3-phenylglycidic acid decarboxylation.

## Conclusions

The decomposition of ethyl and ethyl 3-phenyl glycidate was studied by density functional theory (DFT) and MP2 methods for an accurate study of the nature of the reaction mechanism. The calculations indicate that the first step of the reaction has a six-membered transition state and the reaction proceeds through an asynchronous concerted mechanism. The second step of the mechanism of the decarboxylation of glycidic acid occurs via a five-membered cyclic transition state; the other pathway via a four-membered cyclic transition state proposed for this step by experiments [6] shows Gibbs free energy of activation 22.4 kcal mol<sup>-1</sup> higher than the pathway via a five-membered cyclic transition state at the MP2/6–31+G\* level.

Although the first step of both reactions studied in this work is very similar, significant differences were observed in the second step. The transition state of the decarboxylation of 3-phenylglycidic acid has a special stabilization produced by the phenyl group. Therefore, the rate-determining step for the decomposition of ethyl 3-phenyl glycidate is TS1, while the rate-determining step for the decomposition of ethyl glycidate is TS2.

Evaluation at different calculation levels yielded results that are similar to those described in a previous theoretical study of the thermal elimination of ethyl formate [15]. The

**Table 3** Natural bond orbital (NBO) charges, calculated at the B3LYP/6–31+G\* level, at the atom involved in the reaction center for the rate-determining step for the reaction of the decomposition of ethyl and ethyl 3-phenyl glycidate

| NBO charges              |                |                |                |                |                |                |
|--------------------------|----------------|----------------|----------------|----------------|----------------|----------------|
| Ethyl glycidate          |                |                |                |                |                |                |
|                          | C <sub>1</sub> | O <sub>2</sub> | H <sub>9</sub> | O <sub>5</sub> | C <sub>4</sub> | C <sub>3</sub> |
| react                    | -0.13          | -0.55          | 0.52           | -0.71          | 0.77           | -0.07          |
| TS2                      | -0.01          | -0.64          | 0.54           | -0.66          | 0.78           | -0.14          |
| Ethyl 3-phenyl glycidate |                |                |                |                |                |                |
|                          | O <sub>5</sub> | C <sub>4</sub> | O <sub>6</sub> | C <sub>7</sub> | C <sub>8</sub> | H <sub>9</sub> |
| react                    | -0.60          | 0.78           | -0.55          | -0.14          | -0.72          | 0.25           |
| TS1                      | -0.68          | 0.79           | -0.63          | -0.11          | -0.82          | 0.42           |

use of a method including electronic correlation and diffuse basis set is fundamental for a good description of the studied systems.

Theoretical results for activation energy show good agreement with experimental values. The calculated percentages of evolution of the bonds involved in the reaction indicate that O<sub>6</sub>–C<sub>7</sub> bond breaking for ethyl 3-phenyl glycidate and H<sub>9</sub>–O<sub>5</sub> bond breaking for ethyl glycidate are the most advanced processes for the reactions in the transition states.

**Acknowledgments** The authors want to express their gratitude to the Centro de Supercomputación de Galicia (CESGA) for the use of their computers. D.J. thanks the Spanish Ministry of Education for “Formación de Profesorado Universitario (FPU)” scholarship.

## References

1. Dullaghan ME, Nord FF (1953) *J Org Chem* 18:878–881
2. Blanchard EP, Buchi G (1963) *J Am Chem Soc* 85:955–958
3. Shiner VJ, Martin B (1962) *J Am Chem Soc* 84:4824–4827
4. Singh SP, Kagan J (1970) *J Org Chem* 35:2203–2207
5. Newman MS, Magerlein BJ (2011) The Darzens glycidic ester condensation. In: *Organic reactions*, Wiley, New York, pp 413–440
6. Chuchani G, Tosta M, Rotinov A, Herize A (2004) *J Phys Org Chem* 17:694–698
7. Notario R, Quijano J, Sánchez C, Vélez E (2005) *J Phys Org Chem* 18:134–141
8. Chuchani G, Nuñez O, Marcano N, Napolitano S, Rodríguez H, Ascanio J, Rotinov A, Domínguez RM, Herize A (2001) *J Phys Org Chem* 14:146–158
9. Mirna M, Heredia R, Loroño M, Córdova T, Chuchani G (2006) *J Mol Struct (THEOCHEM)* 770:131–137
10. Quijano C, Notario R, Quijano J, Sánchez C, León L, Vélez E (2003) *Theor Chem Acc* 110:377–386
11. Hölderich WF, Barsnick B (2001) Rearrangement of epoxides. In: Sheldon SA, von Bekkum H (eds) *Fine chemicals through heterogeneous catalysis*. Wiley-VCH, Mannheim, pp 217–231
12. Janes D, Kantar D, Kreft S, Prosen H (2009) *Food Chem* 112:120–124
13. Tieman D, Schauer N, Fernie AR, Hanson AD, Klee HJ (2006) 103:8287–8292
14. Wiberg KB (1968) *Tetrahedron* 24:1083–1096
15. Hermida-Ramón JM, Rodríguez-Otero J, Cabaleiro-Lago EM (2003) *J Phys Chem A* 107:1651–1654
16. Fukui K (1970) *J Phys Chem* 74:4161–4163
17. Frisch MJ, Trucks GW, Schlegel HB, Scuseria GE, Robb MA, Cheeseman JR, Montgomery JA, Vreven T, Kudin KN, Burant JC, Millam JM, Iyengar SS, Tomasi J, Barone V, Mennucci B, Cossi M, Scalmani G, Rega N, Petersson GA, Nakatsuji H, Hada M, Ehara M, Toyota K, Fukuda R, Hasegawa J, Ishida M, Nakajima T, Honda Y, Kitao O, Nakai H, Klene M, Li X, Knox JE, Hratchian HP, Cross JB, Bakken V, Adamo C, Jaramillo J, Gomperts R, Stratmann RE, Yazyev O, Austin AJ, Cammi R, Pomelli C, Ochterski JW, Ayala PY, Morokuma K, Voth GA, Salvador P, Dannenberg JJ, Zakrzewski VG, Dapprich S, Daniels AD, Strain MC, Farkas O, Malick DK, Rabuck AD, Raghavachari K, Foresman JB, Ortiz JV, Cui Q, Baboul AG, Clifford S, Cioslowski J, Stefanov BB, Liu G, Liashenko A, Piskorz P, Komaromi I, Martin RL, Fox DJ, Keith T, Al-Laham MA, Peng CY, Nanayakkara A, Challacombe M, Gill PMW, Johnson B, Chen W, Wong MW, Gonzalez C, Pople JA (2004) *Gaussian 03*, revision C.02. Gaussian Inc, Wallingford
18. Moyano A, Pericàs MA, Valentí EA (1989) *J Org Chem* 54:573–582
19. Domingo LR, Picher MT, Safont VS, Andrés J, Chuchani G (1999) *J Phys Chem A* 103:3935–3943